NOTES AND CORRESPONDENCE

Extracting Envelopes of Rossby Wave Packets

ALEKSEY V. ZIMIN

Department of Physics, University of Maryland, College Park, Maryland

ISTVAN SZUNYOGH

Institute for Physical Science and Technology, and Department of Meteorology, University of Maryland, College Park, Maryland

D. J. PATIL

Institute for Physical Science and Technology, Department of Mathematics, and Department of Meteorology, University of Maryland, College Park, Maryland

BRIAN R. HUNT

Institute for Physical Science and Technology, and Department of Mathematics, University of Maryland, College Park, Maryland

EDWARD OTT

Institute for Research in Electronics and Applied Physics, Department of Physics, and Department of Electrical and Computer Engineering, University of Maryland, College Park, Maryland

29 April 2002 and 5 August 2002

ABSTRACT

Packets of Rossby waves play an important role in the transfer of kinetic energy in the extratropics. The ability to locate, track, and detect changes in the envelope of these wave packets is vital to detecting baroclinic downstream development, tracking the impact of the analysis errors in numerical weather forecasts, and analyzing the forecast effects of targeted weather observations. In this note, it is argued that a well-known technique of digital signal processing, which is based on the Hilbert transform, should be used for extracting the envelope of atmospheric wave packets. This technique is robust, simple, and computationally inexpensive. The superiority of the proposed algorithm over the complex demodulation technique (the only technique previously used for this purpose in atmospheric studies) is demonstrated by examples. The skill of the proposed algorithm is also demonstrated by tracking wave packets in operational weather analyses from the National Centers for Environmental Prediction (NCEP) and analyzing the effects of targeted observations from the 2000 Winter Storm Reconnaissance (WSR00) field program.

1. Introduction

In this note we consider a situation in which we are given a spatially dependent scalar atmospheric quantity $v(x)$, and that there is a range of wavenumbers $0 < k_{\min} \leq k \leq k_{\max}$ in which waves of physical interest are known to occur. Using this information, we seek to extract from $v(x)$ a suitable wavelike component of the form

$$w(x) = A(x)\cos[\phi(x)], \tag{1}$$

where $A(x)$, the envelope, is slowly varying in x as compared to the phase $\phi(x)$ (see Fig. 1 for an example). Often $A(x)$ will be spatially localized, in which case we refer to it as the *wave packet* envelope (for more details see Pedlosky 1987).

The desire to locate wave packets in observed atmospheric data is as old as the knowledge that Rossby waves play a key role in shaping the weather in the midlatitude extratropics (Rossby 1945, 1949; Yeh 1949; Phillips 1990; Persson 2000). The first technique that was used to detect the propagation of synoptic-scale Rossby waves (wavenumbers 4–9) was the trough–ridge

Corresponding author address: Aleksey V. Zimin, Dept. of Physics, University of Maryland, Physics Bldg., Box 240, College Park, MD 20742.
E-mail: alekseyz@physics.umd.edu

© 2003 American Meteorological Society

Unauthenticated | Downloaded 03/31/23 06:11 AM UTC

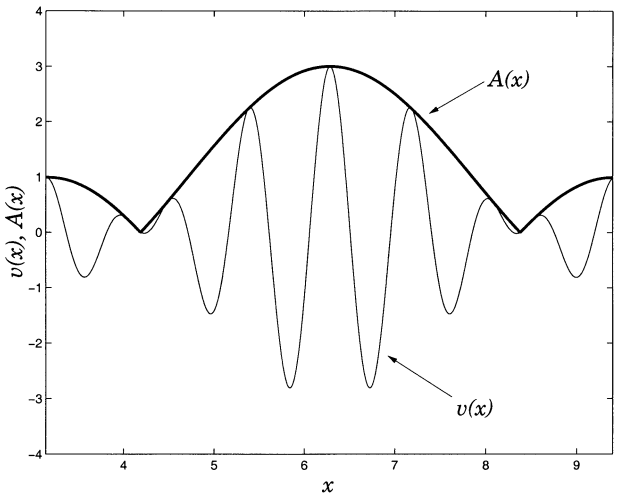

FIG. 1. An analytical example of a wave packet (for details see example 1). Thin line represents the scalar function $\upsilon(x)$ and thick line represents the envelope $A(x)$.

diagram proposed by Hovmöller (1949). In a Hovmöller diagram a selected atmospheric variable, usually the deviation from the mean of the meridional component of the wind or the geopotential height, is averaged over a latitude band and plotted as a time–longitude diagram. The signature of a propagating wave packet in the Hovmöller diagram is a series of alternating positive and negative regions aligned in a diagonal direction.

While the Hovmöller diagram is a powerful tool, it cannot detect the two-dimensional horizontal structure of the wave packets. This can lead to obscure results when wave packets coexist in close proximity at different latitudes. To remedy this problem, recent papers on downstream wave packet propagation (Lee and Held 1993; Chang and Yu 1999; Chang 2000) have utilized the method of *complex demodulation* (for an in-depth review see Bloomfield 2000). This technique assumes that $\upsilon(x)$ can be written as $\upsilon(x) = \mathrm{Re}[A(x)\exp(ikx)]$, where k is a supposed carrier wavenumber. Then the spectrum of $\upsilon(x)$ is shifted by multiplying $\upsilon(x)$ by $\exp(-ikx)$. Finally, the absolute value of the wave packet envelope, $|A(x)|$, is extracted by low-pass filtering to remove high-wavenumber components from the shifted signal. The general wisdom has been that the result is not sensitive to the choice of the carrier wavenumber when it is chosen from a plausible wavenumber range. (For instance, for carrier wavenumber 7 the position and amplitude of the maximum of $|A(x)|$ is usually identified with acceptable precision, even if the demodulation is done by wavenumber 6 or 8.) While this assumption leads to reasonable results in most cases, demodulating by the wrong wavenumber results in incorrect computation of the wave packet envelope when wave packets of distinct carrier wavenumbers coexist at the same latitude.

The aforementioned problem can be easily demonstrated by an example using the following artificial signal that consists of two wave packets with carrier wavenumbers 4 and 9 at the same latitude (see Fig. 2):

$$\upsilon(x) = \exp[-(x-4.5)^2]\cos(4x) + \exp[-(x-7.5)^2]\cos(9x), \qquad \pi \le x \le 3\pi. \tag{2}$$

Figure 2 shows the resulting wave packet envelopes when the demodulation is performed using carrier wavenumbers from 4 through 11. It is evident that demodulating by a single wavenumber distorts the envelope of at least one of the wave packets.

The main aim of this note is to introduce a robust technique for extracting the envelope of atmospheric wave packets that is not affected by the aforementioned problem. The proposed technique does not require the specification of a carrier wavenumber, is easy to implement, and is computationally inexpensive. Although this technique is well known in digital signal processing (Gabor 1946; Oppenheim and Schafer 1975; Laine and Fan 1996), to the best of our knowledge, it has not previously been used for extracting the envelope of atmospheric wave packets. In what follows, we give a step-by-step description of the algorithm (section 2) and demonstrate its skill using four examples (section 3). These examples include two analytical cases for which the packet envelope is known: the tracking of an upper-tropospheric wave packet in operational weather analyses from the National Centers for Environmental Prediction (NCEP), and the tracking of the impact of targeted dropsonde observations that were collected by one of the flight missions during the 2000 Winter Storm Reconnaissance Program (Szunyogh et al. 2002).

2. Description of the algorithm

In what follows, $\upsilon(x)$ is considered on an equidistant grid along a latitude circle, which is parameterized by x, with $0 < x \le 2\pi$. The grid points are located at $x = 2\pi l/N$, where $l = 1, 2, \ldots, N$, and N is an even integer.

The following algorithm is proposed to isolate the wave packet envelopes:

- Step 1. The Fourier transform of the real function $\upsilon(x)$ is computed:

$$\hat{\upsilon}_k = \frac{1}{N}\sum_{l=1}^{N} \upsilon\left(\frac{2\pi l}{N}\right) e^{-2\pi i k l/N}, \qquad \left(k = -\frac{N}{2}+1, \ldots, \frac{N}{2}\right). \tag{3}$$

- Step 2. The inverse Fourier transform is applied to a selected band ($0 < k_{\min} \le k \le k_{\max}$) of the positive wavenumber half of the Fourier spectrum:

$$w\left(\frac{2\pi l}{N}\right) = 2\sum_{k=k_{\min}}^{k_{\max}} \hat{\upsilon}_k e^{2\pi i k l/N}. \tag{4}$$

Unauthenticated | Downloaded 03/31/23 06:11 AM UTC

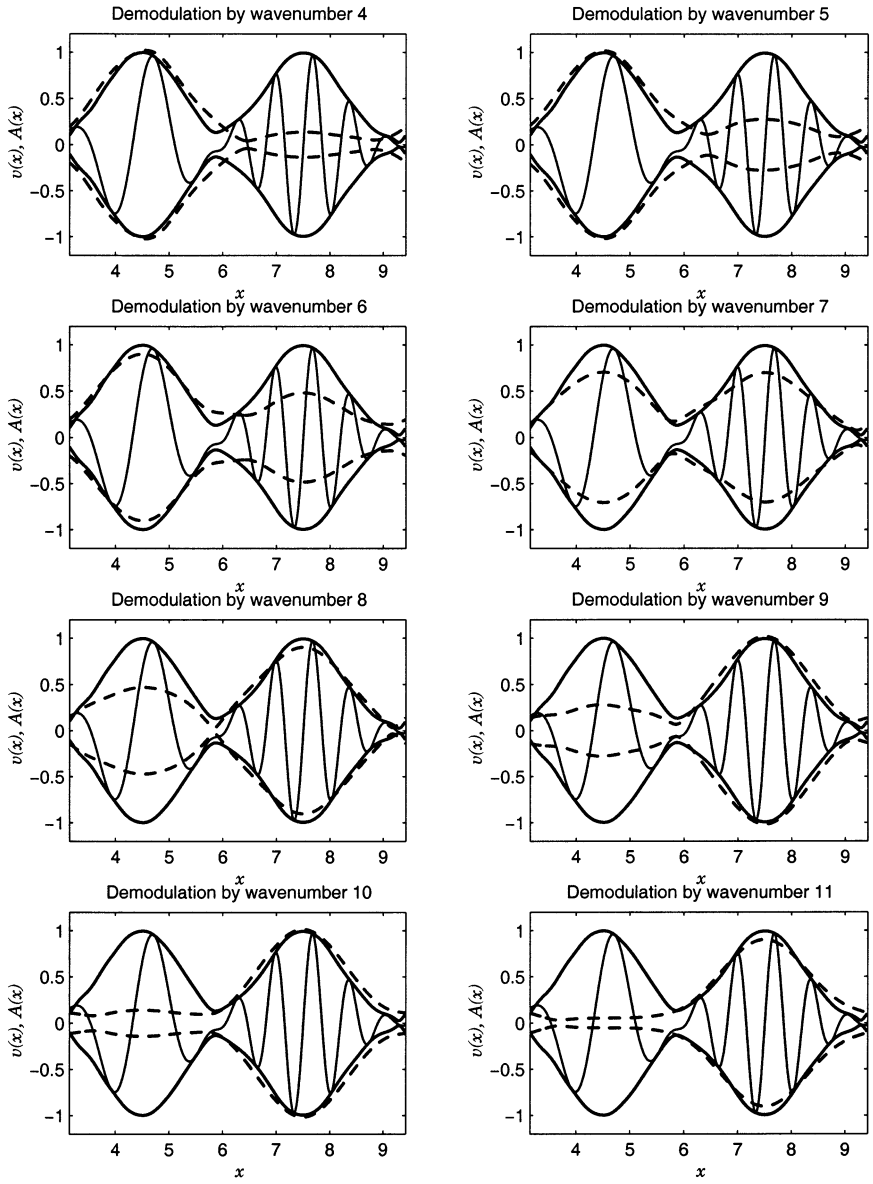

FIG. 2. An analytical example of a function, $\upsilon(x)$, that consists of two wave packets with carrier wavenumbers 4 and 9, respectively. Thin line represents $\upsilon(x)$, while dashed lines show the result of demodulation by wavenumbers from 4 through 11. Thick solid lines represent the envelope recovered by our method.

• Step 3. The packet envelope is computed as follows:

$$A(2\pi l/N) = |w(2\pi l/N)|. \quad (5)$$

This algorithm is a combination of the signal processing technique known as the *Hilbert transform*,[1] and a simple filter that retains only the relevant wavenumber components. Equation (4) also can be viewed as a wavelet transform in which the wavelet is the inverse Fourier transform $f(x)$ of the function $\hat{f}(k)$ shown in Fig. 3a, which is $f(x) \sim [\sin(\Delta k x)/x] \exp(-i\bar{k}x)$, where $\Delta k = (k_{\max} - k_{\min})/2$ and $\bar{k} = (k_{\max} + k_{\min})/2$. A smoother filter (wavelet) might be thought to be more natural, for example, $f(x) \sim [\exp(\Delta k x)^2/2]\Delta k \exp(-i\bar{k}x)$, corresponding to the k-space filter shown in Fig. 3b. We also tested this smoother filter and found that it leads to negligible difference in the results while making the method more complicated.

[1] The Hilbert transform is used in signal processing to recover a complex-valued signal from the real-valued signal by removing the negative wavenumber components from the spectrum of the real signal. If X_r is the real signal, the complex signal can be written as $X = X_r + iH(X_r)$, where $H(\cdot)$ denotes the Hilbert transform.

Unauthenticated | Downloaded 03/31/23 06:11 AM UTC

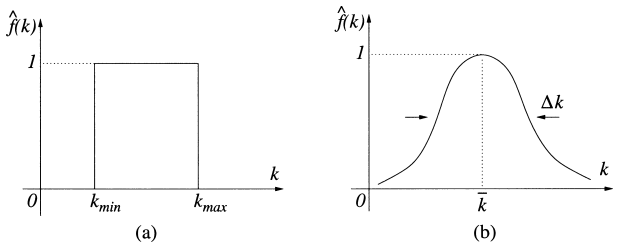

FIG. 3. Two possible choices of the spectral filter function (see section 2 for details).

3. Examples

Example 1: Let

$$v(x) = \cos[(k-1)x] + \cos(kx) + \cos[(k+1)x], \quad x \in [\pi, 3\pi]. \tag{6}$$

Applying steps 1 and 2 of our algorithm, we get $w(x) = \exp[i(k-1)x] + \exp(ikx) + \exp[i(k+1)x]$, and the wave packet envelope for this example is $A(x) = |w(x)| = 1 + 2\cos(x)$. Indeed, $v(x)$ can be expressed in the following form:

$$v(x) = \mathrm{Re}[w(x)] = \mathrm{Re}\{[1 + 2\cos(x)]\exp(ikx)\} = \mathrm{Re}[A(x)\exp(ikx)]. \tag{7}$$

It can be easily verified that $w(x)$ can be obtained numerically by applying the Fourier transform to $v(x)$, removing the negative wavenumber part of the spectrum, and then applying the inverse Fourier transform to the resulting spectrum. The result for $k = 7$ is plotted in Fig. 1.

Example 2: The proposed algorithm is applied to the analytical example, Eq. (2), that was used in section 1 to demonstrate the shortcomings of the complex demodulation technique. For this example we use $k_{\min} = 1$ and $k_{\max} = 12$. Figure 2 shows clearly that, in contrast to complex demodulation, the proposed algorithm accurately extracts the wave packet envelopes when wave packets with different carrier wavenumbers coexist at the same latitude.

Example 3: The proposed algorithm is applied to analyze a case from the 2000 Winter Storm Reconnaissance targeted observations field program (Szunyogh et al. 2002). In particular, we consider the wave packet that significantly contributed to the deepening of a trough over the eastern United States on 25 and 26 January. The most significant failure of the numerical weather prediction models in the 1999–2000 winter season was associated with the prediction of the storm related to this trough (for details see Buizza and Chessa 2002; Langland et al. 2002; Zhang et al. 2002). Our goal is to track the propagation of this upper-tropospheric wave packet. We restrict our analyses to the meridional wind component at the 300-hPa pressure level on a global 2.5° by 2.5° resolution grid ($N = 144$) with 24-h temporal resolution. Since the goal is to track packets of short Rossby waves associated with baroclinic energy conversion, $k_{\min}$ and $k_{\max}$ are chosen to be 4 and 9, respectively. Our wave packet analysis shows clearly why this was a particularly difficult forecast situation. In Fig. 4, the wave packet can be clearly identified even as early as 0000 UTC 21 January 2000 (WP marks the location of the maximum of the packet envelope). At that time the wave packet is located over Japan. Subsequently the hydrodynamical influence in the upper troposphere (and the effect of analysis uncertainties) traveled with the wave packet at an approximate speed of 30° day^{-1} from the Pacific regions. Once the wave packet reached the Atlantic, its envelope started to amplify rapidly due to local baroclinic energy conversion.[2] This result corroborates the conclusions of Langland et al. (2002), obtained by adjoint sensitivity calculations, that initial condition uncertainties over the Pacific had an influence on the quality of the 72-h forecasts of the storm.

Example 4: Studies based on the analytical investigation of idealized atmospheric flows predicted long ago that an initially localized disturbance in the initial condition of a synoptic-scale numerical weather prediction would propagate as a packet of synoptic-scale Rossby waves (Rossby 1949; Charney 1949). Targeted weather observations (e.g., Snyder 1996; Szunyogh et al. 1999; Palmer et al. 1998; Gelaro et al. 1999; Bergot et al. 1999; Pu and Kalnay 1999) change the initial conditions with the aim of removing localized initial condition errors that have potentially large negative forecast effects. As pointed out by Szunyogh et al. (2000, 2002) based on analysis of data from the 1999 and 2000 Winter Storm Reconnaissance programs, upper-tropospheric wave packets play a twofold role in the targeted observation problem. First, they build a dynamical relationship between the targeted region and the verification region, where the forecast is to be improved at a later time. This relationship can be detected by an objective targeting technique, such as the ensemble transform Kalman filter (Bishop et al. 2001). Second, it can be expected that the local changes introduced by the targeted data would propagate in the form of Rossby wave packets in the upper troposphere, as it was predicted by the theory of Rossby (1949) and Charney (1949).

While the results of Szunyogh et al. (2000, 2002) strongly indicated that the latter statement is true even for complex atmospheric flow configurations, no strong evidence was offered to show that the impact of the dropsondes propagates in the form of synoptic-scale Rossby wave packets. One way to demonstrate that this view is correct is to show that the wave packet can be detected in the dropsonde signal. [This signal is defined

[2] Our results on the local energetics of the wave packets are reported in Szunyogh et al. (2002). In that paper, the envelope of the wave packet was extracted by the multiple wavenumber packet identification (MWPI) technique (manuscript is available from the corresponding author), which was an earlier version of the algorithm presented here.

Unauthenticated | Downloaded 03/31/23 06:11 AM UTC

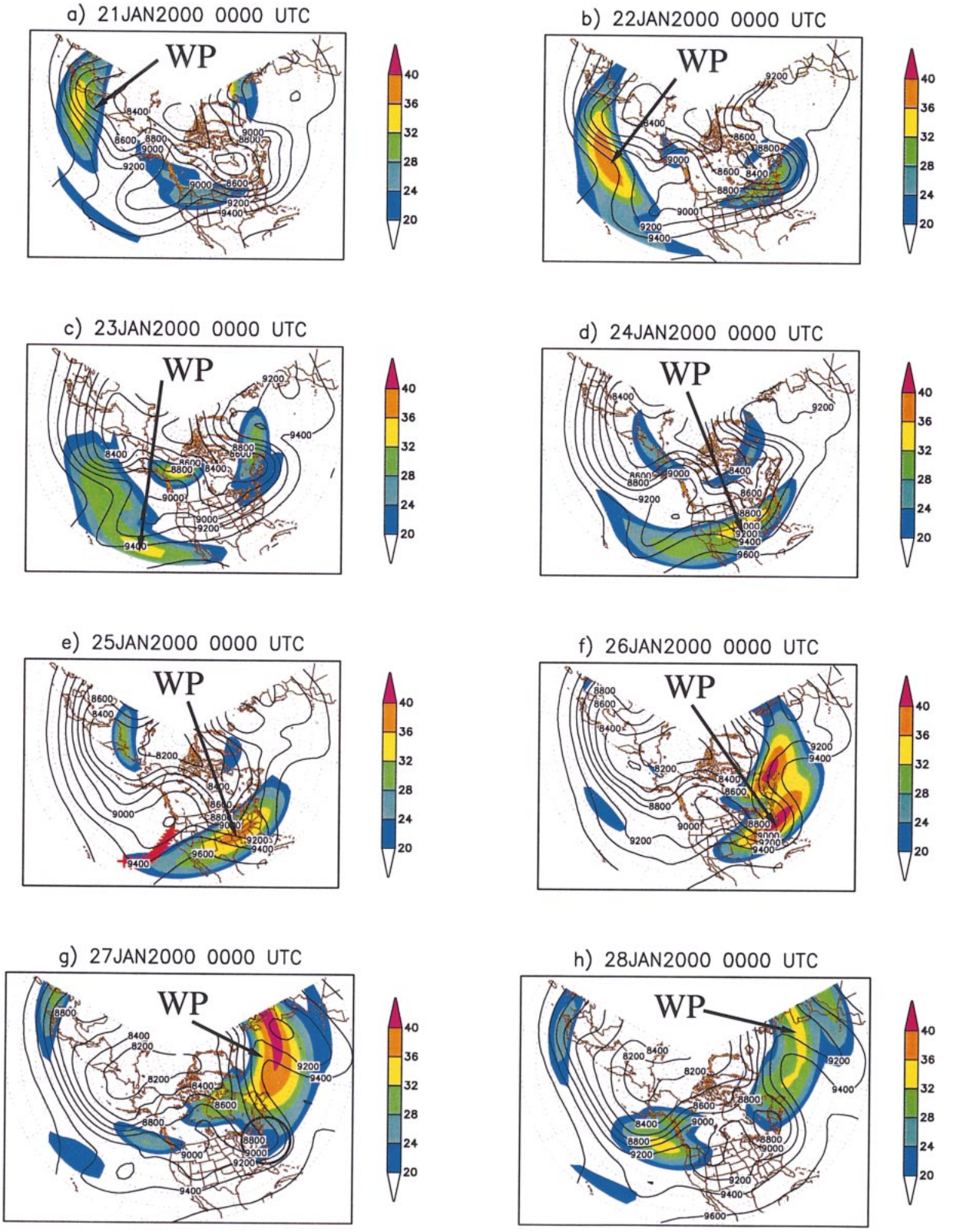

FIG. 4. Time evolution of wave packet envelope $A(x)$ of the meridional wind velocity (m s^{-1}) at 300 hPa for the 8-day period starting at 0000 UTC 21 Jan 2000. Values smaller than 20 m s^{-1} are not shown. Contour lines show the NCEP analysis for the geopotential height at the 300-hPa surface. WP marks the center of the wave packet described in example 3. The dropsonde locations are shown by red crosses at 0000 UTC 25 Jan 2000 and the verification region is marked by a circle at 0000 UTC 27 Jan 2000 (see example 4 for details).

Unauthenticated | Downloaded 03/31/23 06:11 AM UTC

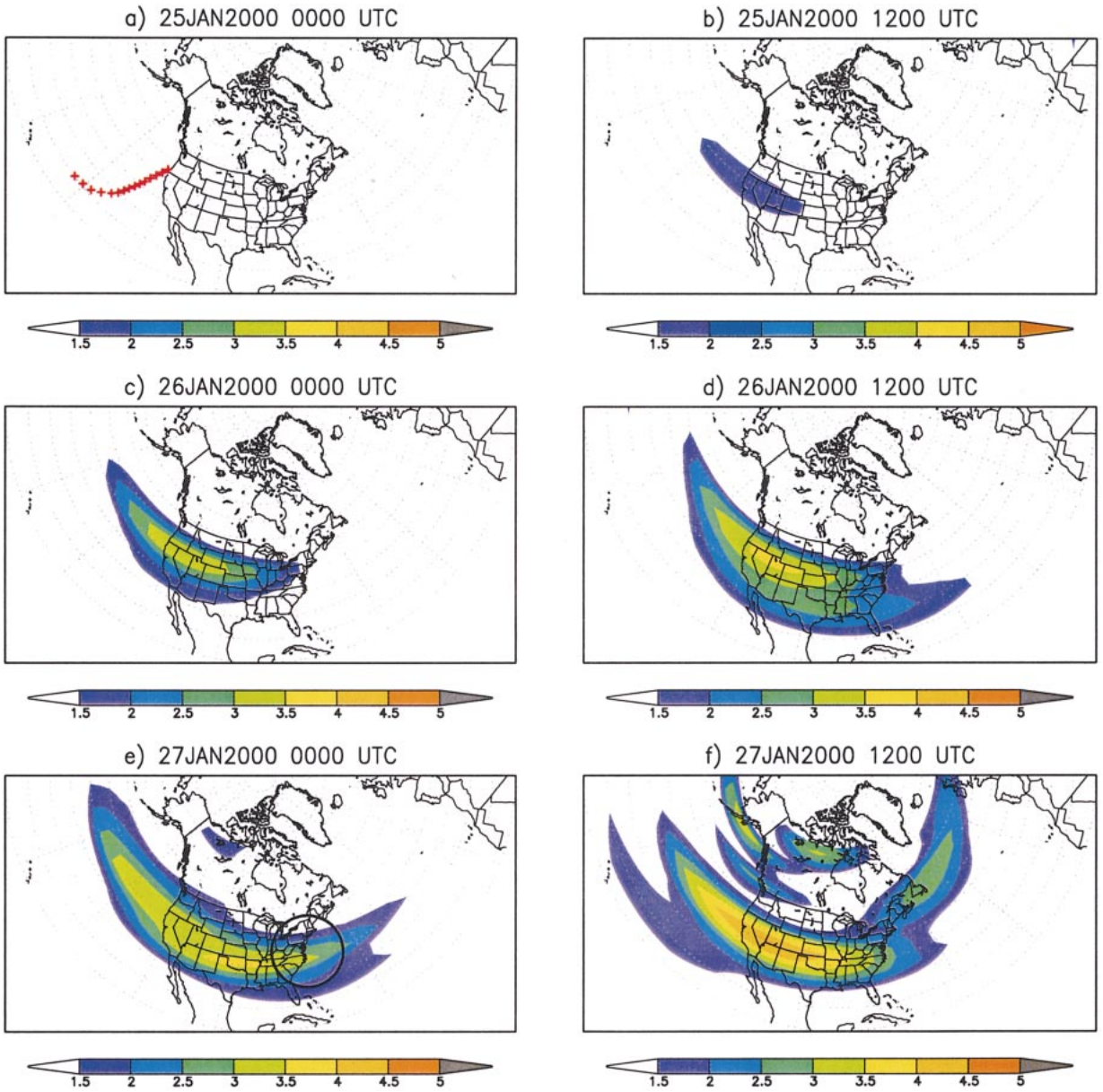

FIG. 5. Time evolution of the envelope of the 300-hPa geopotential height signal (gpm) for the 3-day period starting at 0000 UTC 25 Jan 2000. The signal is defined by the difference between a forecast that was initiated by assimilating all targeted and standard (nontargeted) observations and a forecast that was initiated by assimilating only the standard observations. Values smaller than 1.5 gpm are not shown. The dropsonde locations are shown by red crosses at 0000 UTC 25 Jan 2000 and the verification region is marked by a circle at 0000 UTC 27 Jan 2000.

by the difference between the NCEP global model forecast that was initiated by assimilating all targeted and standard (nontargeted) observations and the NCEP global model forecast that was initiated by assimilating only the standard observations.]

In this example, the algorithm described in section 2 is applied to the signal from a dropsonde mission that was associated with the atmospheric wave packet of example 3. Targeted observations were collected at 0000 UTC 25 January 2000 to improve the prediction of a secondary development at 0000 UTC 27 January 2000 over the East Coast, and not the major storm itself on 25–26 January 2000 (see Szunyogh et al. 2002 for further details). Figure 4 shows that the dropsonde observations targeted the tail of the observed atmospheric wave packet and that the verification region was also located at the tail of the eastward propagating wave packet at verification time. The results shown in Fig. 5 demonstrate that after an initial transient, not longer than 12 h, the data impact in the upper troposphere propa-

Unauthenticated | Downloaded 03/31/23 06:11 AM UTC

gated in the form of a wave packet and the leading edge of the eastward expanding data impact propagated with the speed of the atmospheric wave packet.

4. Conclusions

In this note we have presented a robust objective method for extracting the envelope of packets of synoptic-scale Rossby waves. We believe that our method provides a potentially useful tool in analyzing meteorological problems related to the propagation of wave packets, such as studying local baroclinic instability (Swanson and Pierrehumbert 1994; Orlanski and Sheldon 1993), tracking the origin of localized forecast errors (Persson 2000), and analyzing the propagation of the influence of targeted observations (Szunyogh et al. 2002).

Acknowledgments. The authors are grateful to Dr. Edmund Chang for his careful review of the manuscript. He kindly provided example 2 and his comments aided in our implementation of the complex demodulation technique. This research was supported by the W. M. Keck Foundation, the Office of Naval Research, and the National Science Foundation (Award DMS0104087).

REFERENCES

Bergot, T., G. Hello, and A. Joly, 1999: Adaptive observations: A feasibility study. *Mon. Wea. Rev.,* **127,** 743–765.

Bishop, C. H., B. J. Etherton, and S. J. Majumdar, 2001: Adaptive sampling with the ensemble transform Kalman filter. Part I: Theoretical aspects. *Mon. Wea. Rev.,* **129,** 420–436.

Bloomfield, P., 2000: *Fourier Analysis of Time Series: An Introduction.* 2d ed. Wiley-Interscience, 261 pp.

Buizza, R., and P. Chessa, 2002: Prediction of the U.S. storm of 24–26 January 2000 with the ECMWF Ensemble Prediction System. *Mon. Wea. Rev.,* **130,** 1531–1551.

Chang, E. K. M., 2000: Wave packets and life cycles of troughs in the upper troposphere: Examples from the Southern Hemisphere summer season of 1984/85. *Mon. Wea. Rev.,* **128,** 25–50.

——, and D. B. Yu, 1999: Characteristics of wave packets in the upper troposphere. Part I: Northern Hemisphere winter. *J. Atmos. Sci.,* **56,** 1708–1728.

Charney, J. G., 1949: On a physical basis for numerical prediction of large-scale motions in the atmosphere. *J. Meteor.,* **6,** 371–385.

Gabor, D., 1946: Theory of communication. *J. IEEE,* **93,** 429–457.

Gelaro, R., R. H. Langland, G. D. Rohaly, and T. E. Rossmond, 1999: An assessment of the singular-vector approach to target observations using the FASTEX dataset. *Quart. J. Roy. Meteor. Soc.,* **125,** 3299–3328.

Hovmöller, E., 1949: The trough-and-ridge diagram. *Tellus,* **1,** 62–66.

Laine, A., and J. Fan, 1996: Frame representations for texture segmentation. *IEEE Trans. Image Process.,* **5,** 771–780.

Langland, R. H., M. A. Shapiro, and R. Gelaro, 2002: Initial condition sensitivity and error growth in forecasts of the 25 January 2000 East Coast snowstorm. *Mon. Wea. Rev.,* **130,** 957–974.

Lee, S., and I. M. Held, 1993: Baroclinic wave packets in models and observations. *J. Atmos. Sci.,* **50,** 1413–1428.

Oppenheim, A., and R. Shafer, 1975: *Digital Signal Processing.* Prentice Hall, 585 pp.

Orlanski, I., and J. P. Sheldon, 1993: A case of downstream baroclinic development over western North America. *Mon. Wea. Rev.,* **121,** 2929–2950.

Palmer, T. N., R. Gelaro, J. Barkmeijer, and R. Buizza, 1998: Singular vectors, metrics, and adaptive observations. *J. Atmos. Sci.,* **55,** 633–653.

Pedlosky, J., 1987: *Geophysical Fluid Dynamics.* 2d ed. Springer-Verlag, 710 pp.

Persson, A., 2000: Synoptic–dynamic diagnosis of medium range weather forecast systems. *Proc. of the Seminars on Diagnosis of Models and Data Assimilation Systems,* Reading, United Kingdom, ECMWF, 123–137.

Phillips, N. A., 1990: *Dispersion Processes in Large-Scale Weather Prediction.* WMO-No. 700, World Meteorological Organization, 126 pp.

Pu, Z.-X., and E. Kalnay, 1999: Targeting observations with the quasi-inverse linear and adjoint NCEP global models: Performance during FASTEX. *Quart. J. Roy. Meteor. Soc.,* **125,** 3329–3337.

Rossby, C.-G., 1945: On the propagation of frequencies and energy in certain types of oceanic and atmospheric waves. *J. Meteor.,* **2,** 187–204.

——, 1949: On the dispersion of planetary waves in a barotropic atmosphere. *Tellus,* **1,** 54–58.

Snyder, C., 1996: Summary of an informal workshop on adaptive observations and FASTEX. *Bull. Amer. Meteor. Soc.,* **77,** 953–961.

Swanson, K., and R. T. Pierrehumbert, 1994: Nonlinear wave packet evolution on a baroclinically unstable jet. *J. Atmos. Sci.,* **51,** 384–396.

Szunyogh, I., Z. Toth, K. A. Emanuel, C. H. Bishop, C. Snyder, R. E. Morss, J. Woolen, and T. Marchok, 1999: Ensemble-based targeting experiments during FASTEX: The effect of dropsonde data from the Lear jet. *Quart. J. Roy. Meteor. Soc.,* **125,** 3189–3218.

——, ——, R. E. Morss, S. J. Majumdar, B. J. Etherton, and C. H. Bishop, 2000: The effect of targeted dropsonde observations during the 1999 Winter Storm Reconnaissance Program. *Mon. Wea. Rev.,* **128,** 3520–3537.

——, ——, A. V. Zimin, S. J. Majumdar, and A. Persson, 2002: On the propagation of the effect of targeted observations: The 2000 Winter Storm Reconnaissance Program. *Mon. Wea. Rev.,* **130,** 1144–1165.

Yeh, T., 1949: On energy dispersion in the atmosphere. *J. Meteor.,* **6,** 1–16.

Zhang, F., C. Snyder, and R. Rotunno, 2002: Mesoscale predictability of the ''surprise'' snowstorm of 24–25 January 2000. *Mon. Wea. Rev.,* **130,** 1617–1632.

Unauthenticated | Downloaded 03/31/23 06:11 AM UTC